Geophysical Research Letters

RESEARCH LETTER
10.1029/2019GL082461

Intensification of the North American Monsoon Rainfall as Observed From a Long-Term High-Density Gauge Network

Eleonora M. C. Demaria[1], Pieter Hazenberg[2], Russell L. Scott[1], Menberu B. Meles[1], Mary Nichols[1], and David Goodrich[1]

[1]USDA-ARS, Southwest Watershed Research Center, Tucson, AZ, USA, [2]Department of Hydrology and Atmospheric Sciences, University of Arizona, Tucson, AZ, USA

Key Points:
- Intensification of subdaily summer monsoon rainfall since the 1970s is observed in southwestern United States
- Unique long-term, high-resolution data set reveals changes in rainfall intensities not seen in gridded data sets or isolated rain gauges
- Spatial extent of monsoon convective storms has not changed with time

Supporting Information:
- Supporting Information S1
- Figure S1
- Figure S2
- Figure S3
- Figure S4
- Figure S5
- Figure S6
- Figure S7
- Figure S8
- Figure S9
- Figure S10

Abstract As the atmosphere gets warmer, rainfall intensification is expected across the planet with anticipated impacts on ecological and human systems. In the southwestern United States and northwestern Mexico, the highly variable and localized nature of rainfall during the North American Monsoon makes it difficult to detect temporal changes in rainfall intensities in response to climatic change. This study addresses this challenge by using the dense, subdaily, and daily observations from 59 rain gauges located in southeastern Arizona. We find an intensification of monsoon subdaily rainfall intensities starting in the mid-1970s that has not been observed in previous studies or simulated with high-resolution climate models. Our results highlight the need for long-term, high spatiotemporal observations to detect environmental responses to a changing climate in highly variable environments and show that analyses based on limited observations or gridded data sets fail to capture temporal changes potentially leading to erroneous conclusions.

Correspondence to:
E. M. C. Demaria,
eleonora.demaria@ars.usda.gov

Citation:
Demaria, E. M. C., Hazenberg, P., Scott, R. L., Meles, M. B., Nichols, M., & Goodrich, D. (2019). Intensification of the North American Monsoon rainfall as observed from a long-term high-density gauge network. *Geophysical Research Letters*, *46*. https://doi.org/10.1029/2019GL082461

Received 13 FEB 2019
Accepted 30 APR 2019
Accepted article online 16 MAY 2019

1. Introduction

Intensification of precipitation extremes is expected as the climate warms and the atmosphere's capacity to hold water increases (Allan & Soden, 2008; Fischer & Knutti, 2016; O'Gorman & Schneider, 2009; Trenberth et al., 2003). Increases in daily rainfall extremes have been reported during the instrumental record at the global and continental scales (Donat et al., 2016; Fischer & Knutti, 2015; Kunkel, 2003; Wasko & Sharma, 2015). There is strong evidence that subdaily intensities in water-limited environments have increased in observations (Panthou et al., 2018; Wasko et al., 2015; Wasko & Sharma, 2015) and climate model simulations (Fischer & Knutti, 2016; Min et al., 2011; Prein et al., 2016). Changes in rainfall intensities are crucial, especially in regions like the southwestern United States where a few high-intensity and short-duration storms are responsible for the majority of the annual precipitation and critical for ecosystem health (Friedman & Lee, 2002; Huxman et al., 2004; Stromberg et al., 2017). Rainfall intensities are also the critical determinant of runoff in semiarid regions that can result in flash floods with devastating consequences for human life (Ashley & Ashley, 2008; Morin et al., 2006; Osborn & Lane, 1969; Saharia et al., 2017; Syed et al., 2003). However, in water-limited regions, substantial spatial rainfall variability can exist across scales of a few kilometers that is not captured by isolated rain gauges or represented within typical climate model computational grids, which can mask the signals of heavy rainfall (Borodina et al., 2017). In the southwestern United States and northwestern Mexico, where most rainfall results from highly localized convective storms from the summertime North American Monsoon (NAM), the natural low-frequency climate variability has led to contradictory findings with respect to trends in rainfall intensities. For instance, statistically significant increases in daily monsoon rainfall over specific periods of record have been reported (Arriaga-Ramirez & Cavazos, 2010; Nichols et al., 2002). However, their analyses did not include the latest drought that began in the mid-1990s (Scott et al., 2015; Udall & Overpeck, 2017). Similarly, increases in daily rainfall with a 20-year return period have been documented during the last half of the twentieth century (Kunkel et al., 2013). In contrast, no statistically significant increases in total rainfall or in storm frequency (Anderson et al., 2009; Goodrich et al., 2008; Keefer et al., 2016; Stillman et al., 2013) or decreasing trends (Muschinski & Katz, 2013) have been reported for the region. It is worth pointing out that periods of droughts and pluvials are expected in the NAM region, so temporal trends need to be carefully interpreted in the context of the time period of record. A recent study suggest that observed rainfall intensities in

southeastern Arizona have decreased in the second half of the twentieth century (Singer & Michaelides, 2017) and that those decreases might negatively impact ephemeral river runoff. However, that analysis did not include the most recent drier conditions (Woodhouse et al., 2010).

Climate model simulations of the NAM are challenged by the coarse model spatial resolution that does not allow for a detailed representation of convective processes that often leads to contradictory and unreliable simulations (Tripathi & Dominguez, 2013). For instance, decreases in summer rainfall of ~40% have been simulated with a coarse resolution model (0.5° land and atmosphere grid; Pascale et al., 2017), while high-resolution simulations using a convective-permitting (4-km) model simulations showed increases/decreases in intense rainfall events in the last 60 years in southwestern/southeastern Arizona, respectively (Luong et al., 2017). Since the model spatial and temporal resolution can dramatically influence the projected positive changes in extreme precipitation that are projected for the region (USGCRP, 2017) and those changes are difficult to validate due to the limited availability of long-term observational records, the scientific community for climate studies often relies on heavily interpolated, gridded rainfall data sets that are based on sparse network of rain gauges. Barbero et al. (2017) showed that trends in rainfall extremes are more easily detected in daily rather than in hourly time series, perhaps because of the limited spatial extent of summer storms in the NAM region (Syed et al., 2003). Thus, assessing temporal changes in rainfall intensities in the NAM region requires working at subdaily temporal scales and from a network of rain gauges able to successfully capture the spatial characteristics of monsoon storms. To address this need, in this study, we evaluate the temporal and spatial changes in subdaily and daily NAM rainfall intensities in southeastern Arizona. We compare the results obtained using observations from a dense network of rain gauges for a 57-year (1961–2017) study period with daily gridded and point rainfall from two independent data sets.

2. Data and Analysis

The Walnut Gulch Experimental Watershed (WGEW), now part of the Long-Term Agroecosystem Research network (Kleinman et al., 2018), was established in the 1950s by the United States Department of Agriculture (USDA) Agricultural Research Service (ARS) to support soil and water research in a semiarid environment (Figure 1). With an area of 149 km^2, WGEW is equipped with a rich network of rain gauges (approximately one gauge per 1.5 km^2) to accurately capture the characteristics of the highly localized NAM storms (supporting information Text S1). Average summer rainfall, May through September, over the watershed for the 1961–2017 period has been approximately 293 mm (112- to 370-mm range), which represents approximately 60% of the annual total (Figure 1a). Summer storms frequently occur early in the afternoon (Goodrich et al., 2008; Stillman et al., 2013). Summertime total rainfall anomalies show decadal-scale variability with generally wetter-than-average conditions in the 1960s, 1980s, and 2010s and drier-than-average summers beginning in the 1970s, 1990s, and 2000s (Figure 1c). Average annual temperature is 17.7 °C, and it has steadily increased on average 0.22 °C per decade during the 57 years (Figure 1d). In addition to the WGEW data set, 18 grids from the ~6-km resolution gridded daily precipitation product by Livneh et al. (2013) (hereafter Livneh), and 16 rain gauges from the Global Historical Climatology Network (GHCN; Menne et al., 2012) data set are used for the analysis (supporting information Text S1).

Summer subdaily and daily rainfall intensities over the study period are obtained from breakpoint observations available at 59 rain gauges. Subdaily data are first interpolated to 1-min time steps and then binned into larger duration intervals $D = 0.5$, 1, 1.5, 2, and 24 hr. Daily values are included to compare the results with the Livneh and GHCN data sets. For each day with nonzero totals, the maximum rainfall intensity (I_o) for each D is selected using a moving window over 24 hr. Additionally, hourly data are interpolated into a regular 100 × 100-m grid using a multiquadric-biharmonic interpolation method (Garcia et al., 2008).

Two approaches are used to generate time series of I_o: annual maximum series (AMS) and partial duration series (PDS). To create the AMS time series, the largest I_o is selected for each D and year. For the PDS approach, all I_o values that exceeded the 95th percentile are included in the time series. The 95th percentile value (assumed invariant in time in a nonstationary climate) is computed for all nonzero intensities at each individual gauge which results in an average sample size of 1.6 events per year (supporting information Text S2 and Figure S1). Percentiles ranging from the 90th to the 98th have been used to define what constitutes an

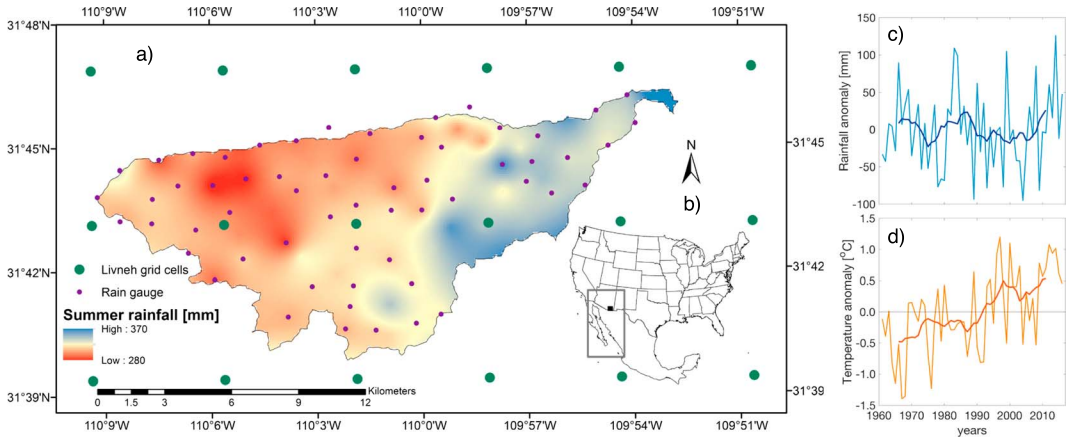

Figure 1. (a) Total summer rainfall, rain gauges, and Livneh grid nodes included in the study. (b) Geographic location of the Walnut Gulch Experimental Watershed and approximate spatial extent of the North American Monsoon region (rectangle). Anomalies, from the 1961–2017 climatology, in watershed average summer (c) rainfall and (d) temperature. Darker lines show the 11-year running mean.

extreme event (Begueria et al., 2011; Groisman et al., 2005; Villarini et al., 2013). A 24-hr window is imposed between events to ensure the statistical independence of PDS rainfall intensities.

The presence and magnitude of the trend in I_o is measured with the nonparametric Mann-Kendall test and Sen's method (Kendall, 1948; Mann, 1945; Sen, 1968) at a 5% and 10% significance level. Additionally, a running-trend analysis with a 30-year time window starting at 1961 is used to assess the impact of time series length and starting year on trend magnitude. Trends are computed at the beginning of each time window. Therefore, the last trend value plotted for 1988 corresponds to the period 1988–2017. Trends in I_o are computed for watershed average values to reduce the uncertainty introduced from the high natural variability of rainfall (Fischer & Knutti, 2014; Kunkel, Karl, Easterling, et al., 2013) and to eliminate the impact of spatial correlation (Douglas et al., 2000; Mascaro, 2018). Trends in I_o at each rain gauge are additionally computed to include an estimation of the spatial variability in the trend results. However, due to the close proximity of rain gauges, there is a larger chance of detecting a trend due to a problem known as test multiplicity (Mascaro, 2018).

Changes in I_o for 2-, 5-, and 20-year return periods (T) are computed with the nonparametric extreme precipitation index (EPI, Janssen et al., 2014; Kunkel et al., 2003). The EPI values for each D are chosen with an empirical threshold associated with the return periods using a partial duration series approach. The threshold is determined as the number of years in the record divided by T (e.g., for the 57 years of record and a 2-year T, the threshold is 29) and used to select the top ranked events. A generalized extreme value and a generalized Pareto function were fitted to the AMS and PDS time series, respectively (supporting information S1). Changes (Δ) are estimated as

$$\Delta = \left\lfloor \frac{X_i - \overline{X}}{\overline{X}} \right\rfloor \times 100, \quad (1)$$

where X represents the variable of interest, the subscript i represents the year, and the bar represents the mean value for the period of interest. All changes are evaluated with the Wilcoxon-Mann-Whitney nonparametric test (Wilks, 1935) at a 5% significance.

Besides looking at temporal changes of watershed average I_o, the study also assesses the occurrence of changes in the spatial characteristic of rainfall using spatially interpolated (100 × 100 m) 1-hr rainfall. For each time step, the area of the watershed covered by rainfall equal or larger than 2.5, 7.5, 12.5, 25, and 50 mm is computed by selecting the grid cells exceeding those thresholds. The thresholds are chosen to cover the whole range of observed rainfall, ranging from 0 to 90 mm. The mean area covered by storms above a given threshold is computed for each year. Note that this method includes rainfall cells that might not be connected in space. Results are compared with the ones from point measurements by computing the number of times observations exceeded the thresholds in each of the 59 rain gauges.

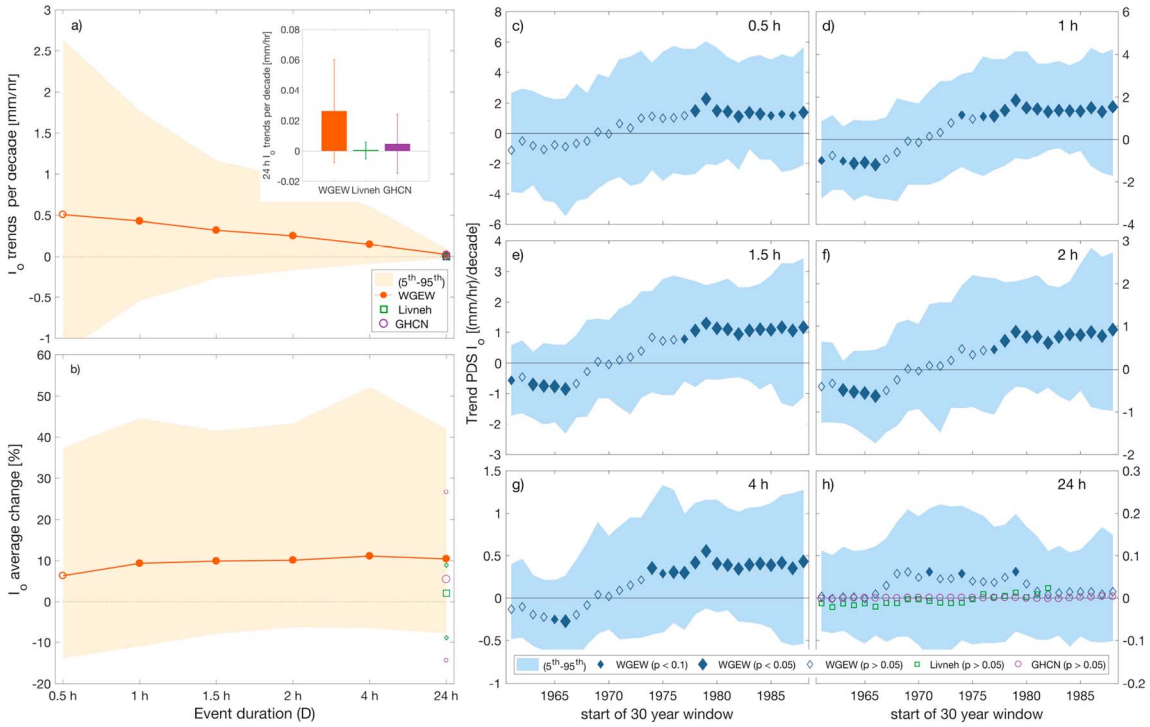

Figure 2. Trend analysis of PDS I_o exceeding the 95th percentile: (a) watershed average trend magnitude; (b) average changes in I_o between the beginning/end years; (c–h) 30-year I_o running trends for different *D*s. The shaded band represents the trend magnitude 5th and 95th percentiles from the 59 rain gauges. Livneh/GHCN trends are indicated in green/purple. Filled symbols denote statistically significant trends. The inset in (a) shows 24-hr average trends ± 1 standard deviation. GHCN = Global Historical Climatology Network; WGEW = Walnut Gulch Experimental Watershed.

3. Results and Discussion

The mean of rainfall intensities exceeding the 95th percentile have been increasing during 1961–2017 period for all durations longer than 1 hr at a rate of 0.50 to 0.03 mm/hr per decade for the 0.5- to 24-hr *D*s, respectively (Figure 2a). Trends are also found to be statistically significant for intensities above the 90th percentile (Figure S3). Shorter durations show larger spatial variability, evident in the 5–95% spread, which indicates the difficulty of drawing accurate conclusions from subdaily trend analyses using a single rain gauge record. The Livneh and GCHN data set show smaller, not significant trend magnitudes of 0.0005 and 0.005 mm/hr per decade, respectively. The inset summarizes daily rainfall intensities from the three data sets. The I_o average changes between the 2017 and 1961 are linked to *D*, with the shortest duration intensity (0.5 hr) increasing by 6% and the longest duration (24 hr) increasing by 11% (Figure 2b). Changes in the Livneh and GHCN data sets are smaller 0.5% and 3.4%, respectively. Positive, albeit not significant, trends in the average frequency of events above the threshold are observed, and decreasing trends in the day of year and time of the day when maximum intensities occurred, on average, indicate storms occurring earlier in the day and in the season (supporting information S1 and Figure S4).

Trend magnitudes computed with a 30-year moving window (Figures 2c–2h) are negative prior to the mid-1960s, and they become positive, and statistically significant, for durations shorter than 4 hr in the mid-1970s. The trends in daily rainfall intensities in the Livneh and GHCN data sets are smaller in magnitude and not statistically significant. The running trend approach allows incorporating into the analysis natural rainfall interannual variability (Figure 1c; e.g., periods below the historical mean in the 1970s, mid-1990s, and early 2000s), as rainfall intensities still show increasing trends despite lower-than-average rainfall totals observed during the most recent and warmer decades. Similar increasing trends, though not statistically significant, are found for the whole study period for the AMS time series (Figures S5 and S6a). The running trend analysis indicates statistically significant positive increases for short durations (1 to 2 hr), starting in the 1980s (Figures S4c–S4h). Our results contradict the results obtained by Singer and Michaelides (2017) using a shorter time series of rainfall from the same network and by Luong et al. (2017) and Pascale et al.

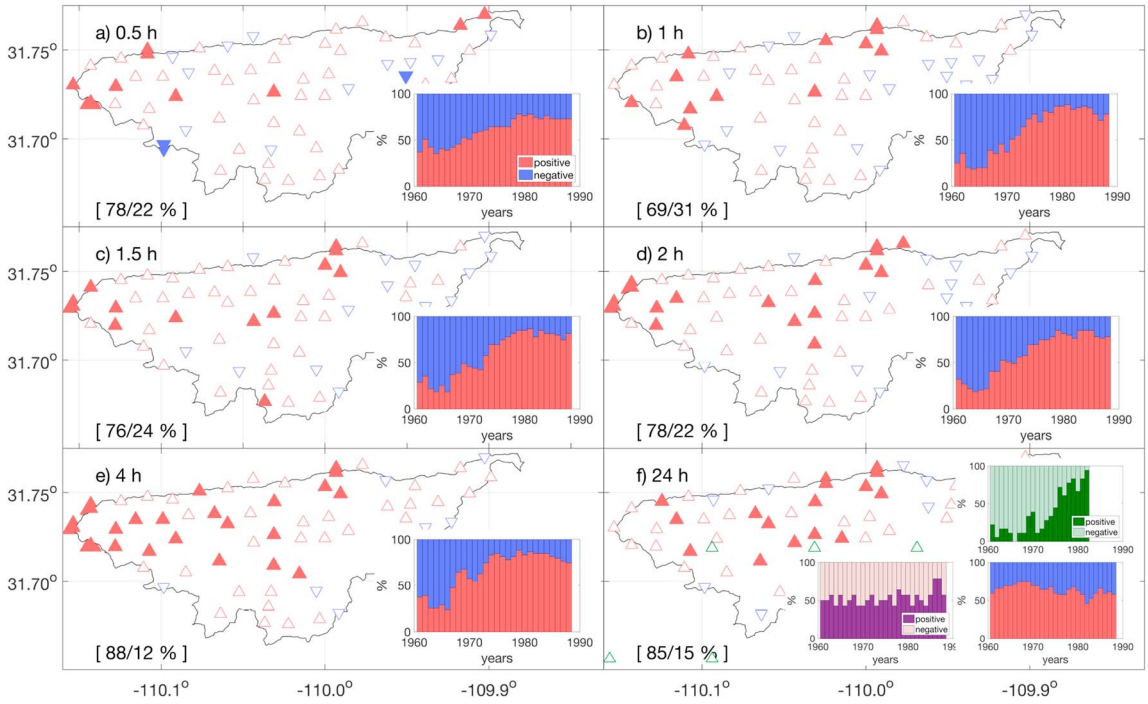

Figure 3. Spatial distribution of trends for the study period (map). The percentage of rain gauges with positive/negative trends is shown between brackets. The insets show percentage of rain gauges with positive/negative 30-year running trends. The Livneh/GHCN data sets are shown in green/purple in panel (f), respectively. Filled symbols denote statistically significant trends (10% level).

(2017) using climate and regional model simulations that suggested no changes or decreases in rainfall intensities in southeastern Arizona. However, the intensification of rainfall with warmer temperatures agrees with what has been found in observations of other semiarid regions (Panthou et al., 2018; Wasko & Sharma, 2015) and in climate models in the United States (Prein et al., 2016). The increase in daily rainfall intensities in semiarid environments since the 1970s has been reported in the Sahelian region in Africa by Panthou et al. (2018). The high noise-to-signal ratio of monsoon rainfall in the region makes the detection of climatic changes a challenge if the length of the observational record is not long enough or the number of observations are limited. For shorter records, the length of the time series itself can be a dominant factor in identification of trends in rainfall intensities, that is, the impact of decadal oscillations on trend analysis of hydroclimatic variables (Chen & Grasby, 2009).

Figure 3 shows the spatial distribution of I_o long-term trends and 30-year running trends for the PDS time series. For the whole study period, the map in each panel shows that between 69% and 88% of the rain gauges have increasing trends across the watershed for different *D*s. Trends obtained with the Livneh data set are also positive but not statistically significant. The 30-year moving-window trend analysis indicates that predominantly positive trends started in the 1970s (bar plot insets in Figure 3) when the number of rain gauges reporting positive trends, albeit not always statistically significant, surpasses 50% (see also Figures 2c–2h). Similar results are found for the AMS time series (Figure S6) with 78% to 90% of the rain gauges observing positive trends during the study period. The Livneh daily rainfall shows the positive trends starting in the mid-1970s, while the GHCN data set fails to capture these trends due to its coarse spatial resolution that has been argued to be one of the reasons why trends are not detected in the United States (Barbero et al., 2017). The fact that some rain gauges report negative trends confirms the highly variable and localized nature of monsoon storms in the region, and it also highlights how crucial it is to use a dense network of rain gauges to characterize temporal changes in convective storm properties since analysis from isolated rain gauges can yield erroneous conclusions.

To evaluate changes in rainfall extremes for different *T*s, the EPI nonparametric measure is evaluated for two 28-year subperiods: 1961–1988 and 1990–2017. Changes in EPI between the two subperiods are sensitive to the duration of the rainfall event and to the return period (Table 1). For the 2-year *T*, positive changes

Table 1
Percentage Changes in Extreme Precipitation Index Between 1961–1988 and 1990–2017 for Different Durations (D) and Return Periods (T)

D (hr)	T (years) 2	5	20
0.5	3.6**	1.4	4.9*
1	1.6	0.6	6.9*
1.5	1.2	0.2	5.9*
2	1.2	1.4	6.4*
4	3.0	1.6	5.2*
24	0.6	1.9	7.0*

*Statistically significant equal medians at the 5% level. **Statistically significant equal medians at the 10% level.

range from 0.6% to 3.6%, whereas for the less frequent intensities ($T = 20$ years), larger positive changes ranging from 4.9% to 7% indicate an increase in the magnitude of rainfall intensities in the most recent decades. These results suggest large events have become more common. Similar changes were found using the fitted GEV probability function (supporting information Table S1 and Figures S8 and S9).

Using hourly interpolated rainfall, on average 18% (±20%) of the 149-km^2 watershed is covered when rainfall is larger than 2.5 mm and the coverage decreases to 4% (±6%) for 25 mm and 1.4% (±1.3%) for 50 mm. The dispersion of the rainfall coverage, measured by the interquartile range, shows large year-to-year variability (Figure 4a). There has been a positive increase in the median area of the watershed covered by 2.5 and 7.5 mm of rainfall ($p < 0.05$). Conversely, for larger rainfall thresholds, linear trends are not statistically significant indicating that the intensification of subdaily rainfalls is not linked to a detectable increase in storm area (Figures 4c–4e). Differences between the 28-year subperiods show slightly larger medians during the most recent period (Figure 4f); however, the medians are not statistically different at the 5% significance level. Similar results are found using hourly data at each rain gauge (Figure S10). These results suggest a mechanism of redistribution of moisture within

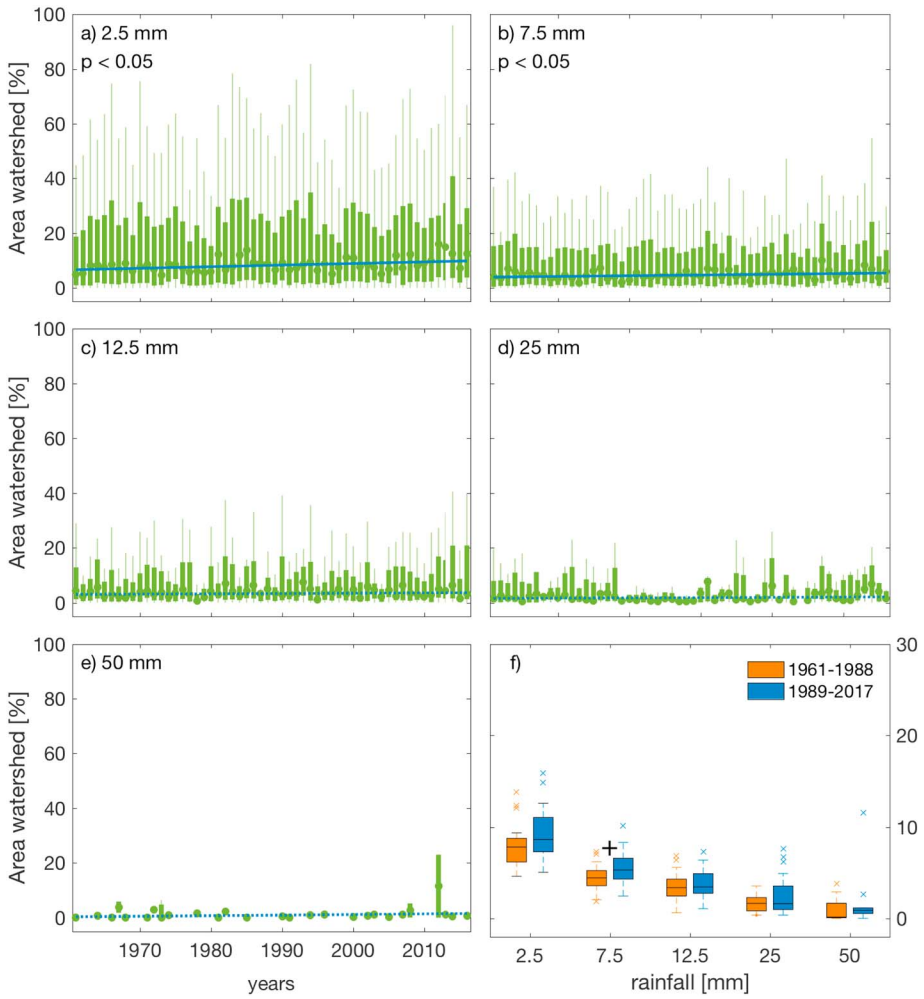

Figure 4. (a–e) Boxplots of changes in mean area of the watershed covered by hourly rainfall exceeding the thresholds. The thick/thin bars show the interquartile/data range. The blue line denotes statistically significant trends ($p < 0.05$). (f) Area coverage for periods 1961–1988 and 1989–2017. The cross indicates equal medians ($p < 0.05$).

storms since more intense rainfall is not linked to larger storm cells as it has been reported by Wasko et al. (2016) in semiarid Australia.

4. Conclusions

It is widely documented that extreme rainfall increases with rising atmospheric temperatures around the world, but how this affects highly variable, in time and space, convective thunderstorms like those found in the NAM region is not well understood thus leading to contradictory results. One of the main roadblocks in the estimation of changes in rainfall intensities in these regions is the lack of sufficiently dense rain gauge networks that can capture the spatiotemporal characteristics of the localized convective monsoon storms. This roadblock limits interpretations of trends in rainfall intensities to data collected from a few scattered rain gauges or to simulations using climate models. Based on observations from a network of 59 rain gauges located in the 149-km^2 WGEW in southeastern Arizona, this study finds clear evidence of an intensification in summer rainfall intensities in the region beginning in the 1970s across a wide range of subdaily timescales. These results contrast with previous climate model simulations and analysis of shorter records of observation, which suggested no changes or even decreases in rainfall intensities in the region (Luong et al., 2017; Singer & Michaelides, 2017). Gridded daily rainfall intensities from Livneh et al. (2013) data set and those from the GHCN stations failed to capture the trends due to their coarse spatial and temporal resolution. As monsoon storm intensities are getting stronger with warmer temperatures, no temporal changes in the storm spatial extent were found. The results therefore confirm the need for dense rain gauge networks observing rainfall at subdaily time steps to characterize changes in convective storm intensity, like those that occur in the NAM region.

Acknowledgments
We thank the group of USDA ARS dedicated staff and technicians for maintaining the rain gauges at WGEW. Thanks to Timothy Keefer, Carl Unkrich, Shea Burns, and Guillermo Ponce-Campos for their help with the data sets. Rainfall data are available at USDA ARS website (https://www.tucson.ars.ag.gov/dap/).

References

Allan, R. P., & Soden, B. J. (2008). Atmospheric warming and the amplification of precipitation extremes. *Science*, *321*(5895), 1481–1484. https://doi.org/10.1126/science.1160787

Anderson, B. T., Wang, J., Gopal, S., & Salvucci, G. (2009). Influence of daily rainfall characteristics on regional summertime precipitation over the southwestern United States. *Journal of Hydrometeorology*, *10*(5), 1218–1230. https://doi.org/10.1175/2009JHM1104.1

Arriaga-Ramirez, S., & Cavazos, T. (2010). Regional trends of daily precipitation indices in northwest Mexico and southwest United States. *Journal of Geophysical Research*, *115*, D14111. https://doi.org/10.1029/2009JD013248

Ashley, S. T., & Ashley, W. S. (2008). Flood fatalities in the United States. *Journal of Applied Meteorology and Climatology*, *47*(3), 805–818. https://doi.org/10.1175/2007JAMC1611.1

Barbero, R., Fowler, H. J., Lenderink, G., & Blenkinsop, S. (2017). Is the intensification of precipitation extremes with global warming better detected at hourly than daily resolutions? *Geophysical Research Letters*, *44*, 974–983. https://doi.org/10.1002/2016GL071917

Begueria, S., Angulo-Martinez, M., Vicente-Serrano, S. M., Ignacio Lopez-Moreno, J., & El-Kenawy, A. (2011). Assessing trends in extreme precipitation events intensity and magnitude using non-stationary peaks-over-threshold analysis: A case study in northeast Spain from 1930 to 2006. *International Journal of Climatology*, *31*(14), 2102–2114. https://doi.org/10.1002/joc.2218

Borodina, A., Fischer, E. M., & Knutti, R. (2017). Models are likely to underestimate increase in heavy rainfall in the extratropical regions with high rainfall intensity. *Geophysical Research Letters*, *44*, 7401–7409. https://doi.org/10.1002/2017GL074530

Chen, Z. H., & Grasby, S. E. (2009). Impact of decadal and century-scale oscillations on hydroclimate trend analyses. *Journal of Hydrology*, *365*(1-2), 122–133. https://doi.org/10.1016/j.jhydrol.2008.11.031

Donat, M. G., Alexander, L. V., Herold, N., & Dittus, A. J. (2016). Temperature and precipitation extremes in century-long gridded observations, reanalyses, and atmospheric model simulations. *Journal of Geophysical Research: Atmospheres*, *121*, 11,174–11,189. https://doi.org/10.1002/2016JD025480

Douglas, E. M., Vogel, R. M., & Kroll, C. N. (2000). Trends in floods and low flows in the United States: Impact of spatial correlation. *Journal of Hydrology*, *240*(1-2), 90–105. https://doi.org/10.1016/S0022-1694(00)00336-X

Fischer, E. M., & Knutti, R. (2014). Detection of spatially aggregated changes in temperature and precipitation extremes. *Geophysical Research Letters*, *41*, 547–554. https://doi.org/10.1002/2013GL058499

Fischer, E. M., & Knutti, R. (2015). Anthropogenic contribution to global occurrence of heavy-precipitation and high-temperature extremes. *Nature Climate Change*, *5*(6), 560–564. https://doi.org/10.1038/nclimate2617

Fischer, E. M., & Knutti, R. (2016). Observed heavy precipitation increase confirms theory and early models. *Nature Climate Change*, *6*(11), 986–991. https://doi.org/10.1038/nclimate3110

Friedman, J. M., & Lee, V. J. (2002). Extreme floods, channel change, and riparian forests along ephemeral streams. *Ecological Monographs*, *72*(3), 409–425. https://doi.org/10.1890/0012-9615(2002)072[0409:EFCCAR]2.0.CO;2

Garcia, M., Peters-Lidard, C. D., & Goodrich, D. C. (2008). Spatial interpolation of precipitation in a dense gauge network for monsoon storm events in the southwestern United States. *Water Resources Research*, *44*, W05S13. https://doi.org/10.1029/2006WR005788

Goodrich, D. C., Unkrich, C. L., Keefer, T. O., Nichols, M. H., Stone, J. J., Levick, L. R., & Scott, R. L. (2008). Event to multidecadal persistence in rainfall and runoff in southeast Arizona. *Water Resources Research*, *44*, W05S14. https://doi.org/10.1029/2007WR006222

Groisman, P. Y., Knight, R. W., Easterling, D. R., Karl, T. R., Hegerl, G. C., & Razuvaev, V. N. (2005). Trends in intense precipitation in the climate record. *Journal of Climate*, *18*(9), 1326–1350. https://doi.org/10.1175/JCLI3339.1

Huxman, T. E., Snyder, K. A., Tissue, D., Leffler, A. J., Ogle, K., Pockman, W. T., et al. (2004). Precipitation pulses and carbon fluxes in semiarid and arid ecosystems. *Oecologia*, *141*(2), 254–268. https://doi.org/10.1007/s00442-004-1682-4

Janssen, E., Wuebbles, D. J., Kunkel, K. E., Olsen, S. C., & Goodman, A. (2014). Observational- and model-based trends and projections of extreme precipitation over the contiguous United States. *Earth's Future*, *2*, 99–113. https://doi.org/10.1002/2013EF000185

Keefer, T. O., Renard, K. G., Goodrich, D. C., Heilman, P., & Unkrich, C. (2016). Quantifying extreme rainfall events and their hydrologic response in southeastern Arizona. *Journal of Hydrologic Engineering*, *21*(1), 04015054. https://doi.org/10.1061/(ASCE)HE.1943-5584.0001270

Kendall, M. G. (1948). *Rank correlation methods* (5th ed., pp. 160). Oxford, England: C. Griffin.

Kleinman, P. J. A., Spiegal, S., Rigby, J. R., Goslee, J. M. B. S. C., Bestelmeyer, B. T., Boughton, R. K., et al. (2018). Advancing the sustainability of US agriculture through long-term research. *Journal of Enviromental Quality*, *47*(6), 1412–1425. https://doi.org/10.2134/jeq2018.05.0171

Kunkel, K. E. (2003). North American trends in extreme precipitation. *Natural Hazards*, *29*(2), 291–305. https://doi.org/10.1023/A:1023694115864

Kunkel, K. E., Easterling, D. R., Redmond, K., & Hubbard, K. (2003). Temporal variations of extreme precipitation events in the United States: 1895-2000. *Geophysical Research Letters*, *30*(17), 1900. https://doi.org/10.1029/2003GL018052

Kunkel, K. E., Karl, T. R., Brooks, H., Kossin, J., Lawrimore, J. H., Arndt, D., et al. (2013). Monitoring and understanding trends in extreme storms state of knowledge. *Bulletin of the American Meteorological Society*, *94*(4), 499–514. https://doi.org/10.1175/BAMS-D-11-00262.1

Kunkel, K. E., Karl, T. R., Easterling, D. R., Redmond, K., Young, J., Yin, X. G., & Hennon, P. (2013). Probable maximum precipitation and climate change. *Geophysical Research Letters*, *40*, 1402–1408. https://doi.org/10.1002/grl.50334

Livneh, B., Rosenberg, E. A., Lin, C., Nijssen, B., Mishra, V., Andreadis, K. M., et al. (2013). A long-term hydrologically based dataset of land surface fluxes and states for the conterminous United States: Update and extensions. *Journal of Climate*, *26*(23), 9384–9392. https://doi.org/10.1175/JCLI-D-12-00508.1

Luong, T. M., Castro, C. L., Chang, H. I., Lahmers, T., Adams, D. K., & Ochoa-Moya, C. A. (2017). The more extreme nature of North American Monsoon precipitation in the southwestern United States as revealed by a historical climatology of simulated severe weather events. *Journal of Applied Meteorology and Climatology*, *56*(9), 2509–2529. https://doi.org/10.1175/JAMC-D-16-0358.1

Mann, H. B. (1945). Nonparametric tests against trend. *Econometrica*, *13*(3), 245–259. https://doi.org/10.2307/1907187

Mascaro, G. (2018). On the distributions of annual and seasonal daily rainfall extremes in central Arizona and their spatial variability. *Journal of Hydrology*, *559*, 266–281. https://doi.org/10.1016/j.jhydrol.2018.02.011

Menne, M. J., Durre, I., Vose, R. S., Gleason, B. E., & Houston, T. G. (2012). An overview of the global historical climatology network-daily database. *Journal of Atmospheric and Oceanic Technology*, *29*(7), 897–910. https://doi.org/10.1175/JTECH-D-11-00103.1

Min, S.-K., Zhang, X., Zwiers, F. W., & Hegerl, G. C. (2011). Human contribution to more-intense precipitation extremes. *Nature*, *470*(7334), 378–381. https://doi.org/10.1038/nature09763

Morin, E., Goodrich, D. C., Maddox, R. A., Gao, X. G., Gupta, H. V., & Sorooshian, S. (2006). Spatial patterns in thunderstorm rainfall events and their coupling with watershed hydrological response. *Advances in Water Resources*, *29*(6), 843–860. https://doi.org/10.1016/j.advwatres.2005.07.014

Muschinski, T., & Katz, J. I. (2013). Trends in hourly rainfall statistics in the United States under a warming climate. *Nature Climate Change*, *3*(6), 577–580. https://doi.org/10.1038/nclimate1828

Nichols, M. H., Renard, K. G., & Osborn, H. B. (2002). Precipitation changes from 1956 to 1996 on the Walnut Gulch Experimental Watershed. *Journal of the American Water Resources Association*, *38*(1), 161–172. https://doi.org/10.1111/j.1752-1688.2002.tb01543.x

O'Gorman, P. A., & Schneider, T. (2009). The physical basis for increases in precipitation extremes in simulations of 21st-century climate change. *Proceedings of the National Academy of Sciences of the United States of America*, *106*(35), 14,773–14,777. https://doi.org/10.1073/pnas.0907610106

Osborn, H. B., & Lane, L. (1969). Precipitation-runoff relations for very small semiarid rangeland watersheds. *Water Resources Research*, *5*(2), 419–425. https://doi.org/10.1029/WR005i002p00419

Panthou, G., Lebel, T., Vischel, T., Quantin, G., Sane, Y., Ba, A., et al. (2018). Rainfall intensification in tropical semi-arid regions: The Sahelian case. *Environmental Research Letters*, *13*(6). https://doi.org/10.1088/1748-9326/aac334

Pascale, S., Boos, W. R., Bordoni, S., Delworth, T. L., Kapnick, S. B., Murakami, H., et al. (2017). Weakening of the North American Monsoon with global warming. *Nature Climate Change*, *7*(11), 806–812. https://doi.org/10.1038/nclimate3412

Prein, A. F., Rasmussen, R. M., Ikeda, K., Liu, C., Clark, M. P., & Holland, G. J. (2016). The future intensification of hourly precipitation extremes. *Nature Climate Change*, *7*, 48.

Saharia, M., Kirstetter, P. E., Vergara, H., Gourley, J. J., & Hong, Y. (2017). Characterization of floods in the United States. *Journal of Hydrology*, *548*, 524–535. https://doi.org/10.1016/j.jhydrol.2017.03.010

Scott, R. L., Biederman, J. A., Hamerlynck, E. P., & Barron-Gafford, G. A. (2015). The carbon balance pivot point of southwestern US semiarid ecosystems: Insights from the 21st century drought. *Journal of Geophysical Research: Biogeosciences*, *120*, 2612–2624. https://doi.org/10.1002/2015JG003181

Sen, P. (1968). Estimates of regression coefficient based on Kendalls tau. *Journal of the American Statistical Association*, *63*(324), 1379–1389. https://doi.org/10.1080/01621459.1968.10480934

Singer, M. B., & Michaelides, K. (2017). Deciphering the expression of climate change within the Lower Colorado River basin by stochastic simulation of convective rainfall. *Environmental Research Letters*, *12*(10). https://doi.org/10.1088/1748-9326/aa8e50

Stillman, S., Zeng, X., Shuttleworth, W. J., Goodrich, D. C., Unkrich, C. L., & Zreda, M. (2013). Spatiotemporal variability of summer precipitation in southeastern Arizona. *Journal of Hydrometeorology*, *14*(6), 1944–1951. https://doi.org/10.1175/JHM-D-13-017.1

Stromberg, J. C., Setaro, D. L., Gallo, E. L., Lohse, K. A., & Meixner, T. (2017). Riparian vegetation of ephemeral streams. *Journal of Arid Environments*, *138*, 27–37. https://doi.org/10.1016/j.jaridenv.2016.12.004

Syed, K. H., Goodrich, D. C., Myers, D. E., & Sorooshian, S. (2003). Spatial characteristics of thunderstorm rainfall fields and their relation to runoff. *Journal of Hydrology*, *271*(1-4), 1–21. https://doi.org/10.1016/S0022-1694(02)00311-6

Trenberth, K. E., Dai, A., Rasmussen, R. M., & Parsons, D. B. (2003). The changing character of precipitation. *Bulletin of the American Meteorological Society*, *84*(9), 1205–1218. https://doi.org/10.1175/BAMS-84-9-1205

Tripathi, O. P., & Dominguez, F. (2013). Effects of spatial resolution in the simulation of daily and subdaily precipitation in the southwestern US. *Journal of Geophysical Research: Atmospheres*, *118*, 7591–7605. https://doi.org/10.1002/jgrd.50590

Udall, B., & Overpeck, J. (2017). The twenty-first century Colorado River hot drought and implications for the future. *Water Resources Research*, *53*, 2404–2418. https://doi.org/10.1002/2016WR019638

USGCRP (2017). Climate science special report: Fourth national climate assessment, Rep. (470 pp.). DC, USA.

Villarini, G., Smith, J. A., & Vecchi, G. A. (2013). Changing frequency of heavy rainfall over the central United States. *Journal of Climate*, *26*(1), 351–357. https://doi.org/10.1175/JCLI-D-12-00043.1

Wasko, C., & Sharma, A. (2015). Steeper temporal distribution of rain intensity at higher temperatures within Australian storms. *Nature Geoscience*, *8*(7), 527–529. https://doi.org/10.1038/ngeo2456

Wasko, C., Sharma, A., & Johnson, F. (2015). Does storm duration modulate the extreme precipitation-temperature scaling relationship? *Geophysical Research Letters*, *42*, 8783–8790. https://doi.org/10.1002/2015GL066274

Wasko, C., Sharma, A., & Westra, S. (2016). Reduced spatial extent of extreme storms at higher temperatures. *Geophysical Research Letters*, *43*, 4026–4032. https://doi.org/10.1002/2016GL068509

Wilks, S. S. (1935). On the independence of k sets of normally distributed statistical variables. *Econometrica*, *3*(3), 309–326. https://doi.org/10.2307/1905324

Woodhouse, C. A., Meko, D. M., MacDonald, G. M., Stahle, D. W., & Cooke, E. R. (2010). A 1,200-year perspective of 21st century drought in southwestern North America. *Proceedings of the National Academy of Sciences of the United States of America*, *107*(50), 21,283–21,288. https://doi.org/10.1073/pnas.0911197107